

Simultaneous determination of catechol and hydroquinone based on poly(sulfosalicylic acid)/functionalized graphene modified electrode

Cong Li · Weilu Liu · Yue Gu · Shuming Hao · Xiaoyi Yan · Zhiquan Zhang · Ming Yang

Received: 8 May 2014 / Accepted: 14 July 2014 / Published online: 17 August 2014
© Springer Science+Business Media Dordrecht 2014

Abstract A glassy carbon electrode (GCE) modified with poly(sulfosalicylic acid) (PSA) and poly(diallyldimethylammonium chloride)-graphene (PDDA-GN) was prepared by a simple self-assembly method. The formation of films was ascribed to the electrostatic force between negatively charged PSA and positively charged PDDA-GN as well as the π - π stacking interaction between PSA and PDDA-GN. The as prepared films were characterized by scanning electron microscopy (SEM), Raman spectroscopy and electrochemical methods. Under the optimized condition, the modified GCE showed two well-defined redox waves for catechol (CT) and hydroquinone (HQ) in cyclic voltammetry (CV) with a peak potential separation of 111 mV, which ensured the anti-interference ability of the electrochemical sensor and made simultaneous determination of dihydroxybenzene isomers possible in real samples. The corresponding oxidation currents increased remarkably compared with those obtained at the bare GCE, PSA/GCE and PDDA-GN/GCE, respectively. Differential pulse voltammetry (DPV) was used for the simultaneous

determination of CT and HQ. The anodic peak current of CT was linear in the concentration from 1×10^{-6} to 4×10^{-4} M in the presence of 3×10^{-5} M HQ, and the detection limit was 2.2×10^{-7} M (S/N = 3). At the same time, the anodic peak current of HQ was linear in the concentration from 2×10^{-6} to 4×10^{-4} M in the presence of 2×10^{-5} M CT, and the detection limit was 3.9×10^{-7} M (S/N = 3). The proposed method was applied to simultaneous determination of CT and HQ in tap water with satisfactory results. These results indicated that PSA/PDDA-GN is a promising modified material with great potential in electrocatalysis and electrochemical sensing.

Keywords Self-assembly · Poly(sulfosalicylic acid) · Poly(diallyldimethylammonium chloride)-graphene · Electrocatalysis · Catechol · Hydroquinone

1 Introduction

Catechol (CT) and hydroquinone (HQ) are the two significant isomers of phenolic compounds being widely used in medicines, cosmetics, pesticides, flavoring agents, dye and photography [1]. Due to their high toxicity and low degradability, CT and HQ are considered as environmental pollutants by the US Environmental Protection Agency (EPA) and the European Union (EU) [2]. To date, several techniques including liquid chromatography [3], capillary electrochromatography [4], electrochemiluminescence [5], and spectrophotometry [6] have been applied to the detection of CT and HQ. Compared with other analytical strategies, electrochemical methods are attractive due to the advantages of simple operation, time saving, low cost, free of complicated samples pre-treatment, high sensitivity and excellent selectivity. However, direct determination of

Electronic supplementary material The online version of this article (doi:10.1007/s10800-014-0713-z) contains supplementary material, which is available to authorized users.

C. Li · W. Liu · Y. Gu · S. Hao · X. Yan · Z. Zhang (✉)
College of Chemistry, Jilin University, Changchun 130012,
People's Republic of China
e-mail: zzq@jlu.edu.cn

W. Liu
School of Pharmacy, Shenyang Pharmaceutical University,
Shenyang 110016, People's Republic of China

M. Yang
Department of Breast Surgery, First Hospital, Jilin University,
Changchun 130021, People's Republic of China
e-mail: yangming1967@163.com

these isomers at conventional electrodes such as glassy carbon and gold electrodes is a challenge, because their redox peak potentials are too close to distinguish. Recently, various functionalized materials, including electrospun carbon nanofibers [7], carbon nanoparticle–chitosan composite [8], mesoporous carbon CMK-3 [9], graphene–chitosan composite [10], penicillamine [11], carbon nanotubes (CNT) [12], poly(thionine) [13], layered tungsten sulfide–graphene nanocomposite [14], graphene oxide doped poly(3,4-ethylenedioxythiophene) [15], and poly(brilliant-cresyl blue) [16], were developed for simultaneous determination of CT and HQ. Therefore, it is meaningful to investigate novel electrode materials for the simultaneous determination of dihydroxybenzene isomers.

In this context, significant advantages have been achieved using conducting polymers to develop electrochemical sensors for measuring organic and inorganic compounds. Conducting polymers can be easily prepared as film electrodeposited over different substrates with good homogeneity, chemical stability, and adherence, with the possibility of incorporating different materials to form composites [17]. The thickness and permeability of the polymeric films can be controlled by the potential and current applied. Fabrication of conducting polymer film is flexible, hence, it provides an attractive mean to overcome the problems caused by the solvent evaporation method [18]. Poly(sulfosalicylic acid) has high concentrations of negatively charged surface-functional groups (SO_3^- and COO^-), which has attracted much attention in the determination of roxithromycin [19], adenine, guanine, thymine [20], and dopamine [21], etc. As far as we know, it has not been reported that poly(sulfosalicylic acid) film is used for the determination of CT and HQ.

Graphene (GN) has great attraction as a novel single-atom-thick two-dimensional graphitic carbon electrode material [22] because of their large surface area, high thermal and electrical conductivities, impressive mechanical properties, and low cost [23]. It has been reported that graphene-based electrodes were successfully applied to detect some biological and organic molecules, including dopamine [24], ascorbic acid [25], hydrogen peroxide [26], serotonin [27], L-cysteine [28], epinephrine [29], methyl parathion [30], L-lactic acid [31] etc. However, GN is hydrophobic and tends to form agglomerates which may limit its further applications. An enormous amount of efforts have been concerning on covalent or non-covalent methods to functionalize GN in order to obtain solution-processable GN. Covalent interactions are mostly obtained by doping or chemical reaction with the functional groups which are formed during the synthesis of GN. The former approach partly destroys the GN conjugation system and results in suppression of its intrinsic properties. However, non-covalent interactions via Van der Waals forces,

electrostatic attraction, hydrogen bonding, coordination bonds or π – π stacking interactions mostly preserve the natural properties of GN [32, 33]. As a linear positively charged polyelectrolyte, poly(diallyldimethylammonium chloride) (PDDA) [34] has been found to be an effective material to non-covalently functionalize GN sheets [35]. The use of PDDA both as a reducing agent and a stabilizer resulted in the successful reduction of GO and well-dispersed graphene in aqueous solution. Interestingly, the positively charged PDDA-functionalized graphene (PDDA-GN) has been employed as a matrix to anchor some negatively charged materials for fabricating multifunctional composites [36].

Herein, we prepared poly(sulfosalicylic acid) (PSA) and poly(diallyldimethylammonium chloride)-graphene (PDDA-GN) modified glassy carbon electrode for simultaneous determination of CT and HQ. A layer of PSA film was obtained at a glassy carbon electrode (PSA/GCE) by electrochemical polymerization. The PSA film has high concentrations of negatively charged surface-functional groups (SO_3^- and COO^-) [37], which could effectively increase the adhesion and stability of PDDA-GN layer. Furthermore, the combination of PDDA-GN with PSA will produce some synergistic effects, such as improved mechanical stability, enlarged active surface area and enhanced electric conductivity. CT and HQ exhibited two corresponding, well-defined oxidation peaks with sufficiently differing peak potential and enhanced peak currents at the modified electrode. The proposed method would potentially be applied to multi-component analysis in environmental control and chemical industry.

2 Experimental

2.1 Apparatus

The electrode materials were characterized by field emission scanning electron microscopy (SEM) (Hitachi S-4800) and Raman spectroscopy (Horiba Jobin Yvon T64000 system with 633 nm radiations). Electrochemical measurements were carried out on a CHI660A electrochemical workstation (Shanghai Chenhua). A conventional three-electrode system was employed with a bare or modified GCE (3 mm diameter) as working electrode, a platinum wire as the counter electrode, a saturated calomel electrode (SCE) as the reference electrode. All potentials reported in this paper were referenced to the SCE.

2.2 Chemicals and materials

Natural graphite was purchased from Qingdao Hengrui Industrial, China. Sulfosalicylic acid, catechol and

hydroquinone are all analytical grade from Shanghai Chemical Factory, China. Phosphate buffer solutions (PBS) were prepared by mixing the stock solutions of 0.1 M KH_2PO_4 and 0.1 M Na_2HPO_4 , and then adjusting the pH with HCl and NaOH. $[\text{Fe}(\text{CN})_6]^{3-/4-}/\text{KCl}$ solution (10 mM) was prepared by mixing 0.1 M KCl, 10 mM $\text{K}_3[\text{Fe}(\text{CN})_6]$ and 10 mM $\text{K}_4[\text{Fe}(\text{CN})_6]$. Aqueous solutions were prepared with three distilled water.

2.3 Synthesis of the PDDA-GN and electrode preparation

First, graphene oxide (GO) was synthesized from natural graphite powder by the modified Hummers method [38], then PDDA (20 % in water, 0.2 mL) was added into the homogeneous GO dispersion (0.5 mg mL^{-1} , 20.0 mL). After being sonicated for 30 min, the solution was placed in a household microwave oven for 8 min (power: 600 W. Notice: after continuous heating for 2 min, the microwave oven should stop for a 2-min rest). The product was isolated, and the residual PDDA was removed by centrifugation at 10,000 rpm for 20 min, followed by consecutive washing/centrifugation cycles two times with water. The collected product was redispersed readily in water/ethanol mixture to produce a colloidal PDDA-GN suspension.

Prior to modification, the bare GCE was polished successively with 0.3 and 0.05 μm Al_2O_3 slurry on the tracing paper. Then it was washed successively with 1:1 nitric acid, acetone and water in an ultrasonic bath and dried under a stream of nitrogen. The GCE was immersed in PBS of pH 5.5 containing 10 mM sulfosalicylic acid. By cyclic sweeping from -1.0 to 2.0 V at 100 mV s^{-1} for 25 cycles, the PSA/GCE was obtained. Afterwards, the PSA/GCE was carefully rinsed with doubly distilled water and immersed in PDDA-GN (1 mg mL^{-1}) for 2 h to form the PSA/PDDA-GN/GCE and finally dried by nitrogen. For control experiments, the PSA/GCE was prepared in the same electropolymerization process, and the PDDA-GN/GCE was prepared in the absence of PSA.

3 Results and discussion

3.1 Characterization of PSA/PDDA-GN

SEM was used to surface characterization of PSA/GCE and PSA/PDDA-GN/GCE and the results are presented in Fig. 1a, b. From Fig. 1a, it can be clearly seen that PSA film was a rod-like structure indicating that the film was successfully polymerized on the surface of GCE. The image of PSA/PDDA-GN film, as shown in Fig. 1b, indicated that PDDA-GN was distributed homogeneously on the surface of PSA/GCE. The formation of films was

ascribed to the electrostatic force between negatively charged PSA and positively charged PDDA-GN as well as the π - π stacking interaction between PSA and PDDA-GN.

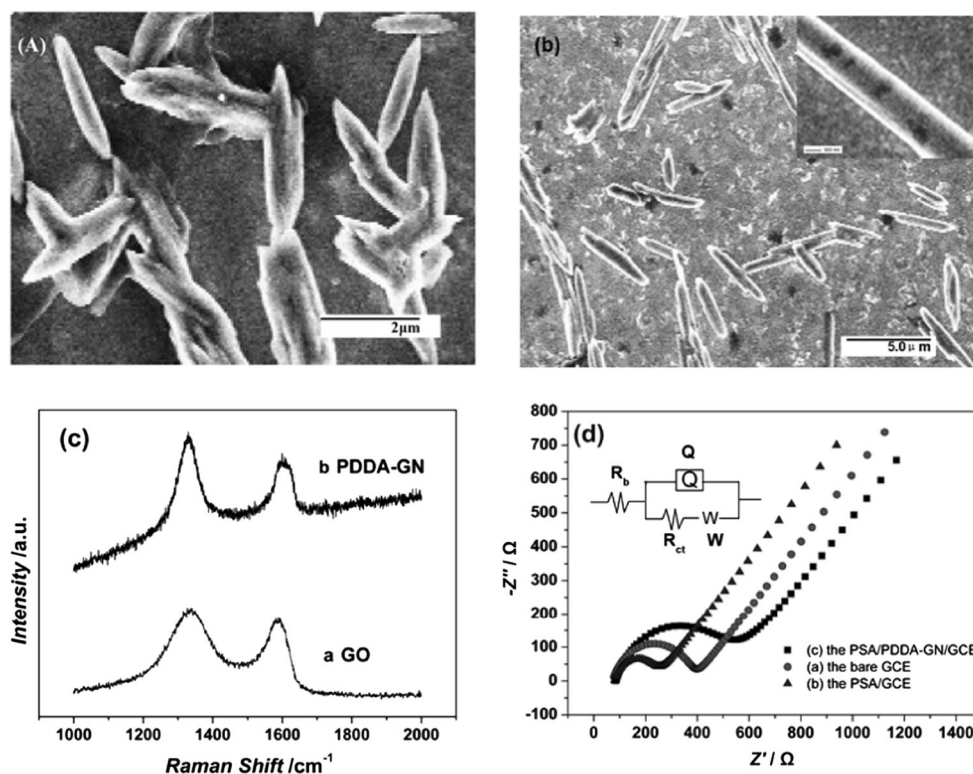
Raman spectroscopy is a powerful tool to characterize the structure and quality of carbonaceous materials, especially for distinguishing ordered structures from disordered structures. G band is usually assigned to the E_{2g} phonon of C sp^2 atoms, while D band is a breathing mode of κ -point phonons of A_{1g} symmetry [39]. Raman spectroscopy (Fig. 1c) for both GO (curve a) and PDDA-GN (curve b) exhibited two remarkable peaks at around 1,330 and $1,598 \text{ cm}^{-1}$, which assigned to the well-defined D band and G band, respectively. The frequencies of the D band and G band in PDDA-GN were similar to those observed in GO. However, PDDA-GN had an increased D/G intensity ratio compared with GO. This change indicates a decrease in the size of the in-plane sp^2 domains and a partially ordered crystal structure of PDDA-GN.

EIS is widely used to investigate the interfacial properties of solid electrodes and solution bulk for information such as electron transfers, electrode impedances, electric double layer, and the surface charge transfer resistance (R_{ct}). The results are usually shown as a semicircular part at higher frequencies corresponds to the kinetic control, and a linear part at lower frequencies corresponds to the mass transfer control. The diameter of the semicircle represents the R_{ct} at the electrode surface while the linear part represents Warburg impedance (Z_w) [40]. The Nyquist plots of 10 mM $[\text{Fe}(\text{CN})_6]^{3-/4-}$ and 0.1 M KCl at bare GCE, PSA/GCE, PSA/PDDA-GN/GCE within the frequency range of 0.01 Hz–100 kHz are shown in Fig. 1d. For the bare GCE (curve a), the R_{ct} value was estimated to be 313.6 Ω . After the electrochemical polymerization of sulfosalicylic acid, the R_{ct} value decreased to 159.5 Ω (curve b), implying PSA played an important role in accelerating the electron transfer between electrode and probe molecules. The value of the PSA/PDDA-GN/GCE increased to 446.6 Ω (curve c), indicating that the PDDA-GN could self-assemble on the PSA/GCE and hindered the electron transfer from the redox probe to the electrode surface. These results demonstrate the successful immobilization of PSA and PDDA-GN.

3.2 Optimization of PSA/PDDA-GN-modified GCE on the response of CT and HQ

A series of cyclic voltammeteries (CVs) were carried out for the polymerization of sulfosalicylic acid on GCE. It is well known that the thickness of the polymer film is directly related to the number of potential cycles during electropolymerization [41]. The effect of film thickness was studied on the response of CT and HQ (Supporting Information Fig. S1). The PSA film was prepared on GCE in pH 5.5

Fig. 1 **a** SEM image of the PSA/GCE **b** SEM image of the PSA/PDDA-GN/GCE **c** Raman spectroscopy of GO (a) and PDDA-GN (b) **d** Electrochemical impedance spectra of bare GCE (a), PSA/GCE (b) and PSA/PDDA-GN/GCE (c) in 10 mM $[\text{Fe}(\text{CN})_6]^{3-/4-}$ and 0.1 M KCl solution. R_b bulk resistance, R_{ct} charge transfer resistance, Q constant phase element (CPE), W Warburg



PBS containing 10 mM sulfosalicylic acid, using cycles ranging from 5 to 35. Figure S1a illustrated the variations in the electrocatalytic nature of the PSA film with the different number of cycles. It can be seen that the oxidation peak current and the reduction peak current of CT and HQ increased with the increasing electrodeposition cycle until the cycle number reached 25. When the electrodeposition cycle increased to more than 25, both the oxidation and reduction peak currents started to decrease. It may be associated with the thickness of PSA film related to the obstruction of electron transfer on the electrode surface [13]. Cycle number 25 during polymerization was therefore considered as the optimum number and was used in further experiments. Moreover, Fig. S1b illustrated the effect of the different immersion time on the electrochemical detection of CT and HQ. It was clear that the current change was inconspicuous, therefore, 2 h was selected.

3.3 Electrochemical oxidation behavior of CT and HQ

Figure 2 depicted the cyclic voltammograms of a mixture of 2.0×10^{-4} M HQ and 2.0×10^{-4} M CT at different electrodes in PBS (pH 3.0). There was only one pair of redox peaks at the bare GCE (curve a), and the redox peaks of CT and HQ overlapped each other. In the case of the PDDA-GN/GCE (curve b), two pairs of peaks were exhibited, which indicated that the oxidation and reduction peaks of CT and HQ can be separated, but the peak

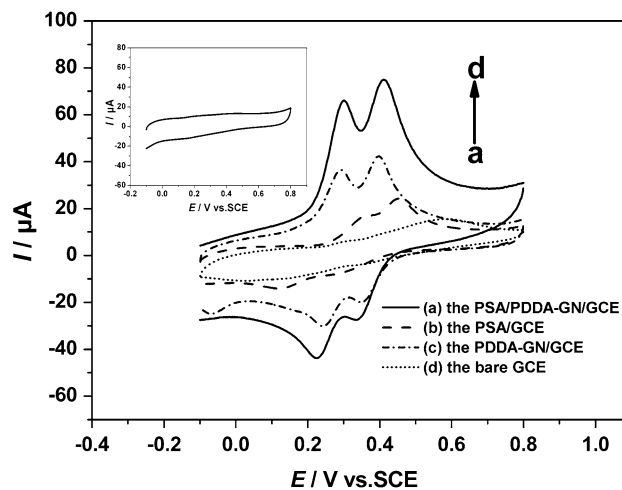
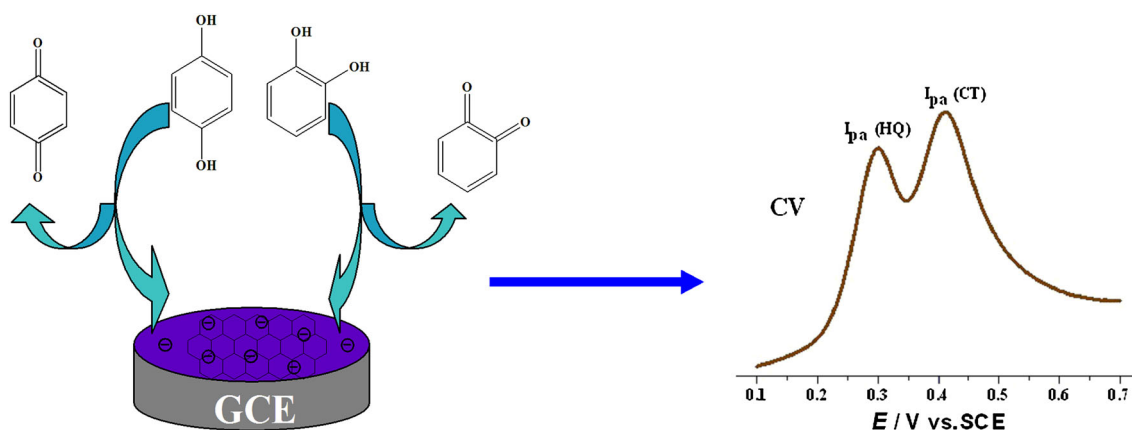


Fig. 2 Cyclic voltammograms of 2.0×10^{-4} M CT and 2.0×10^{-4} M HQ in pH 3.0 PBS at different electrodes. *a* bare GCE, *b* PDDA-GN/GCE, *c* PSA/GCE and *d* PSA/PDDA-GN/GCE. Scan rate: 100 mV s^{-1} . *Inset* Cyclic voltammograms of PSA/PDDA-GN/GCE in pH 3.0 PBS

currents were rather small. However, there were two pairs of well-defined reversible peaks of CT and HQ at the PSA/GCE (curve c). The overpotential of the redox peaks was obviously decreased and the peak currents were improved. Interestingly, at the PSA/PDDA-GN/GCE (curve d), two advantages were found: (1) the peak currents were much stronger than those at the other electrodes. (2) The redox



Scheme 1 Schematic illustration of facilitated charge transport for CT or HQ oxidation by the PSA/PDDA-GN/GCE

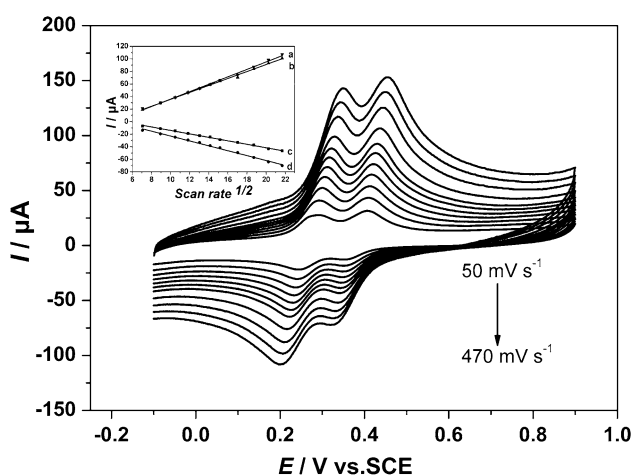


Fig. 3 Cyclic voltammograms at the PSA/PDDA-GN/GCE with different potential scan rates in PBS (pH 3.0) containing a mixture of 2.0×10^{-4} M CT and 2.0×10^{-4} M HQ. The scan rates are 50, 80, 110, 140, 170, 200, 230, 290, 350, 410, 470 mV s^{-1} , respectively. Inset the dependence of the peak current on the square root of scan rates. *a* I_{pa} of CT, *b* I_{pa} of HQ, *c* I_{pc} of CT, *d* I_{pc} of HQ

peaks of CT and HQ can be easily divided. It was found that the oxidation peak potential separation was 111 mV. Therefore, the PSA/PDDA-GN/GCE made the simultaneous and sensitive determination of CT and HQ possible.

The excellent performance of PSA/PDDA-GN/GCE may attribute to the following reasons. Firstly, the hydroxyl, carboxyl and sulfonic groups in PSA/PDDA-GN could interact with the hydroxyl groups in two isomers (CT and HQ) via H-bonding. In the PBS of pH 3.0, the negatively charged PSA [37] could also interact with the positively charged HQ (pKa 9.96) and CT (pKa 9.48) through the favorable electrostatic attraction. These interactions may help to lower the activation energy of the redox reactions required. The overpotential of reactions was therefore decreased. Secondly, the two isomers can be enriched on

PSA/PDDA-GN/GCE due to the large surface area of the PDDA-GN. Thirdly, the good combination between the PDDA-GN and PSA may be favorable for the charge transfer. Facilitation of charge transport of CT or HQ molecules by the PSA/PDDA-GN/GCE is schematically shown in Scheme 1.

3.4 Influence of scan rate

To study the effect of potential sweep rate on the peak current, cyclic voltammetry was recorded at different potential sweep rates in a wide range of 50–470 mV s^{-1} in PBS (pH 3.0) containing 2.0×10^{-4} M HQ and 2.0×10^{-4} M CT on the PSA/PDDA-GN/GCE (Fig. 3). As shown in the inset of Fig. 3, a good linear relationship between the peak current (I) and the square root of the scan rate ($v^{1/2}$) was obtained. This demonstrated that the redox process of CT and HQ at the PSA/PDDA-GN/GCE was controlled by diffusion. The equations for I with $v^{1/2}$ for CT and HQ were expressed as follows:

CT :

$$I_{\text{pa}}(\mu\text{A}) = 5.918 v^{1/2} - 23.268 \quad (v \text{ in } \text{mV s}^{-1}, R = 0.998)$$

$$I_{\text{pc}}(\mu\text{A}) = -3.900 v^{1/2} + 16.033 \quad (v \text{ in } \text{mV s}^{-1}, R = 0.997)$$

HQ :

$$I_{\text{pa}}(\mu\text{A}) = 5.543 v^{1/2} - 19.897 \quad (v \text{ in } \text{mV s}^{-1}, R = 0.998)$$

$$I_{\text{pc}}(\mu\text{A}) = -2.763 v^{1/2} + 13.632 \quad (v \text{ in } \text{mV s}^{-1}, R = 0.999)$$

3.5 Effect of pH on the electrochemical behavior of CT and HQ

The effect of pH value on the electrochemical behavior of 2×10^{-4} M CT and 2×10^{-4} M HQ in the mixed solution at the PSA/PDDA-GN/GCE was carefully investigated by CV in the pH range from 3.0 to 9.0 (Fig. 4a). The inset of Fig. 4b revealed that the largest peak current was

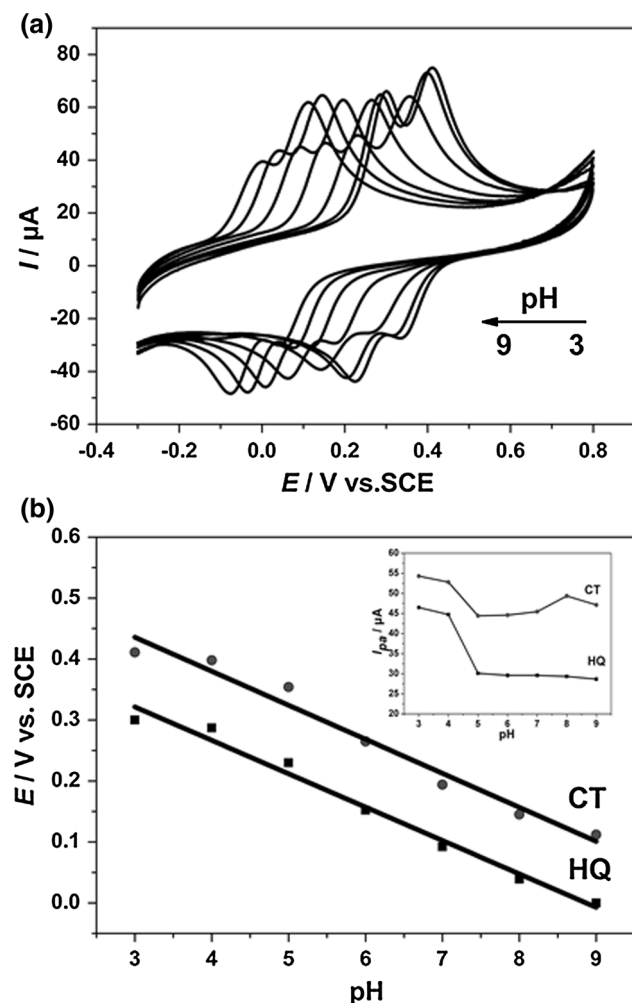


Fig. 4 **a** Cyclic voltammograms of 2.0×10^{-4} M CT and 2.0×10^{-4} M HQ at the PSA/GN/GCE in PBS with different pH. **b** The dependence of the potential on pH. *Inset* the dependence of the oxidation peak current on pH

obtained at pH 3.0. Thus pH 3.0 was chosen as the optimum pH value for the detection of CT and HQ in order to achieve high sensitivity. In addition, the relationship between pH and the anodic peak potential was investigated (Fig. 4b). It was observed that the anodic peak potentials of the two isomers shifted to more negative with the increase of pH in the range of pH 3.0–9.0. The two regression lines were almost parallel, indicating that the peak-to-peak separation between CT and HQ was constant at different pH solutions. The equations for peak potential with pH for CT and HQ were expressed as follows:

$$E_{\text{HQ}} = 54.8 \text{ pH} + 485.9 \text{ (mV, } R = 0.991)$$

$$E_{\text{CT}} = 55.8 \text{ pH} + 603.4 \text{ (mV, } R = 0.986)$$

The slopes of these equations were close to the theoretical value of 59 mV pH^{-1} , suggesting that the redox reaction of CT or HQ at the PSA/PDDA-GN/GCE should be a two

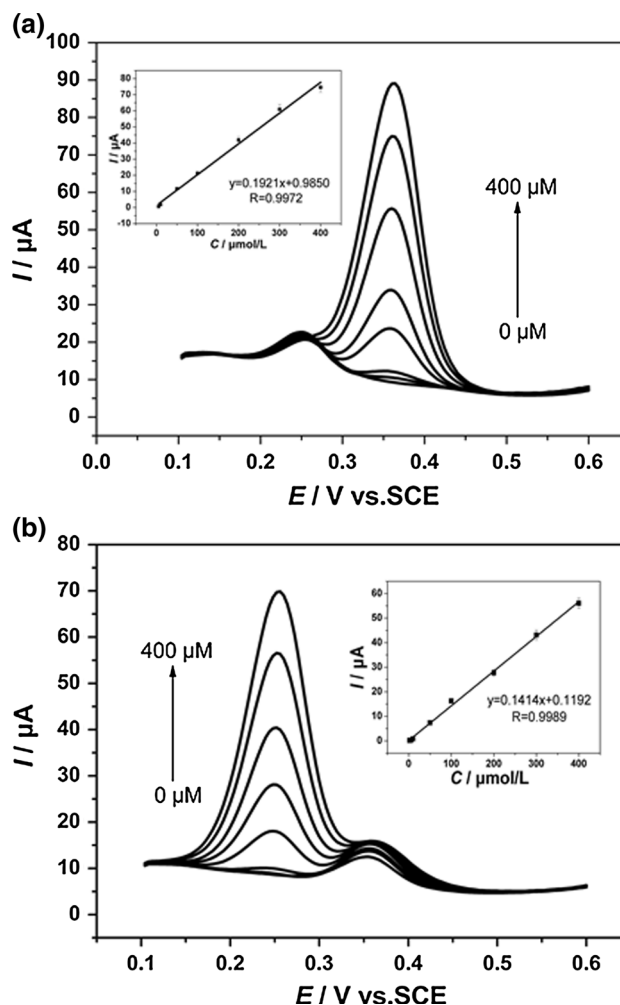


Fig. 5 **a** Differential pulse voltammograms at the PSA/PDDA-GN/GCE in PBS (pH 3.0) containing different concentrations of CT (0 , 1.0×10^{-6} , 5.0×10^{-6} , 1.0×10^{-5} , 5.0×10^{-5} , 1.0×10^{-4} , 2.0×10^{-4} , 3.0×10^{-4} and 4.0×10^{-4} M). The concentration of HQ was kept constant at 3.0×10^{-5} M. *Inset* the dependence of the CT peak currents on concentrations. **b** Differential pulse voltammograms at the PSA/PDDA-GN/GCE in PBS (pH 3.0) containing different concentrations of HQ (0 , 2.0×10^{-6} , 5.0×10^{-6} , 1.0×10^{-5} , 5.0×10^{-5} , 1.0×10^{-4} , 2.0×10^{-4} , 3.0×10^{-4} and 4.0×10^{-4} M). The concentration of CT was kept constant at 2.0×10^{-5} M. *Inset* the dependence of the HQ peak currents on concentrations

electrons and two protons process. This result is consistent with the previous reports [42–44].

3.6 Simultaneous determination of CT and HQ using differential pulse voltammetry

The electrooxidation processes of CT and HQ in the mixture were also investigated by DPV in PBS (pH 3.0) at the PSA/PDDA-GN/GCE. When the concentration of one species changed, the other one was kept constant. Examination of Fig. 5a showed that the peak current of CT increased with an increase in the CT concentration while

Table 1 Performances comparison of PSA/PDDA-GN/GCE with other material modified electrodes in simultaneous determination of CT and HQ

Electrode	Technique	Linear (μM)		LOD (μM)		Sensitivity ($\mu\text{A mM}^{-1} \text{cm}^{-2}$)		Ref.
		CT	HQ	CT	HQ	CT	HQ	
Graphene–chitosan	DPV	1–400	1–300	0.75	0.75	842.8	800	[10]
PCA ^b	DPV	25–175	15–115	0.6	1.0	1514.3	2242.8	[11]
MWNT	DPV	2–100	2–100	0.6	0.6	1714.2	1457.1	[12]
WS ₂ -graphene	DPV	1–100	1–100	0.2	0.1	446.7	372.9	[14]
PEDOT/GO ^c	DPV	2–400	2.5–200	1.6	1.6	–	–	[15]
PSA/PDDA-GN	DPV	1–400	2–400	0.22	0.39	2744.2	2,020	This work

^a Electrospun carbon nanofiber-modified carbon paste electrode
^b Penicillamine
^c Poly(3,4-ethylenedioxythiophene)/graphene oxide

Table 2 Simultaneous determination of HQ and CT in tap water samples

Sample	Added (μM)		Found ^a (μM)		RSD (%)		Recovery (%)	
	HQ	CT	HQ	CT	HQ	CT	HQ	CT
1	30.00	10.00	29.58	9.750	0.48	0.77	98.60	97.50
2	30.00	50.00	29.80	50.67	2.68	2.10	99.35	101.3
3	30.00	100.0	30.18	103.3	1.22	1.05	100.6	103.3
4	10.00	20.00	9.770	19.59	1.04	0.57	97.71	97.96
5	50.00	20.00	51.64	19.73	2.87	2.57	103.3	98.65
6	100.0	20.00	101.4	19.55	2.48	2.63	101.4	97.75

^a Average of five determinations

the concentration of HQ was kept constant ($3 \times 10^{-5} \text{ M}$). From the inset of Fig. 5a, it can be seen that the oxidation peak current of CT was linear with its concentration in the range of 1×10^{-6} – $4 \times 10^{-4} \text{ M}$. The regression equation was $I_{pa} = 0.1921 C + 0.9850$ (μA , 10^{-6} M , $R = 0.9972$), the detection limit for CT was estimated to be $2.2 \times 10^{-7} \text{ M}$ ($S/N = 3$). Similarly as shown in Fig. 5b, keep the concentration of CT concentration constant as $2 \times 10^{-5} \text{ M}$, the oxidation peak current increased linearly with the increasing concentration of HQ in the range of 2×10^{-6} – $4 \times 10^{-4} \text{ M}$. The regression equation was $I_{pa} = 0.1414 C + 0.1192$ (μA , 10^{-6} M , $R = 0.9989$), the detection limit for CT was estimated to be $3.9 \times 10^{-7} \text{ M}$ ($S/N = 3$). A comparison of the proposed method with other electrochemical methods is listed in Table 1.

3.7 Repeatability, stability and interferences

The modified electrode presented a good repeatability and durability. The relative standard deviation (RSD) of the peak current is below 4 % for seven determinations of CT and HQ. The peak currents remain 90 % of their initial values after the modified electrode was kept for one month at room temperature. The possible interferences of some ions were also investigated. The results show that 1,000-fold concentration of Ca^{2+} , Zn^{2+} , Cl^- , CH_3COO^- , NO_3^- , SO_4^{2-} and five-fold concentration of resorcinol have no effect on determination of dihydroxybenzene isomers ($2.0 \times 10^{-4} \text{ M}$).

3.8 Analytical applications

The utilization of the proposed method in real sample analysis was also investigated by direct analysis of CT and HQ in tap water by using DPV technique. The known concentrations of CT and HQ were added to the samples, then the amounts of CT and HQ in the tap water sample were determined by calibration method and the results are summarized in Table 2. The recoveries were 97.5–103.3 % and 97.7–103.3 % for CT and HQ, respectively, which clearly indicates the applicability and reliability of the proposed method.

4 Conclusions

In this work, the electrochemical behavior of CT and HQ was investigated at PSA/PDDA-GN/GCE by cyclic voltammetry and differential pulse voltammetry. Compared with the bare GCE, the PSA/GCE and the PDDA-GN/GCE, the PSA/PDDA-GN/GCE exhibited high electrocatalytic activities towards the oxidation of CT and HQ, which was testified by the remarkably increasing oxidation peak currents and completely separating peak potentials. The advantage could attribute to the synergistic effect of the electrocatalytic property of PSA and PDDA-GN. The fabricated electrode exhibited excellent reproducibility and good stability. In addition, the proposed method was

applied to determine CT and HQ in water samples with satisfactory results. Thus, a sensitive, selective, reproducible and cost-effective electroanalytical method was developed for the discrimination and measurement of dihydroxybenzene isomers, which holds great potential in electrocatalysis and electrochemical sensing.

Acknowledgments This work was supported by the National Natural Science Foundation of China (No. 21375045) and Natural Science Foundation of Jilin Province (No. 20130101118JC).

References

- Wang J, Park JN, Wei XY, Lee CW (2003) Room-temperature heterogeneous hydroxylation of phenol with hydrogen peroxide over Fe^{2+} , Co^{2+} ion-exchanged Na β zeolite. *Chem Commun* 5:628–629
- Xie T, Liu Q, Shi Y, Liu Q (2006) Simultaneous determination of positional isomers of benzenediols by capillary zone electrophoresis with square wave amperometric detection. *J Chromatogr A* 1109(2):317–321
- Cui H, He C, Zhao G (1999) Determination of polyphenols by high-performance liquid chromatography with inhibited chemiluminescence detection. *J Chromatogr A* 855(1):171–179
- Guan N, Zeng Z, Wang Y, Fu E, Cheng J (2000) Open tubular capillary electrochromatography in fused-silica capillaries chemically bonded with macrocyclic dioxopolyamine. *Anal Chim Acta* 418:145–151
- Sun YG, Cui H, Li YH, Lin XQ (2000) Determination of some catechol derivatives by a flow injection electrochemiluminescent inhibition method. *Talanta* 53(3):661–666
- Nagaraja P, Vasantha R, Sunitha K (2001) A new sensitive and selective spectrophotometric method for the determination of catechol derivatives and its pharmaceutical preparations. *J Pharm Biomed Anal* 25(3):417–424
- Guo Q, Huang J, Chen P, Liu Y, Hou H, You T (2012) Simultaneous determination of catechol and hydroquinone using electrospun carbon nanofibers modified electrode. *Sens Actuators B* 163(1):179–185
- Amiri M, Ghaffari S, Bezaatpour A, Marken F (2012) Carbon nanoparticle–chitosan composite electrode with anion, cation, and neutral binding sites: dihydroxybenzene selectivity. *Sens Actuators B* 162(1):194–200
- Yu J, Du W, Zhao F, Zeng B (2009) High sensitive simultaneous determination of catechol and hydroquinone at mesoporous carbon CMK-3 electrode in comparison with multi-walled carbon nanotubes and Vulcan XC-72 carbon electrodes. *Electrochim Acta* 54(3):984–988
- Yin H, Zhang Q, Zhou Y, Ma Q, Liu T, Zhu L, Ai S (2011) Electrochemical behavior of catechol, resorcinol and hydroquinone at graphene–chitosan composite film modified glassy carbon electrode and their simultaneous determination in water samples. *Electrochim Acta* 56(6):2748–2753
- Wang L, Huang PF, Bai JY, Wang HJ, Zhang LY, Zhao YQ (2007) Covalent modification of a glassy carbon electrode with penicillamine for simultaneous determination of hydroquinone and catechol. *Microchim Acta* 158(1–2):151–157
- Qi H, Zhang C (2005) Simultaneous determination of hydroquinone and catechol at a glassy carbon electrode modified with multiwall carbon nanotubes. *Electroanalysis* 17(10):832–838
- Ahammad A, Rahman MM, Xu GR, Kim S, Lee JJ (2011) Highly sensitive and simultaneous determination of hydroquinone and catechol at poly(thionine) modified glassy carbon electrode. *Electrochim Acta* 56(14):5266–5271
- Huang KJ, Wang L, Liu YJ, Gan T, Liu YM, Wang LL, Fan Y (2013) Synthesis and electrochemical performances of layered tungsten sulfide–graphene nanocomposite as a sensing platform for catechol, resorcinol and hydroquinone. *Electrochim Acta* 107:379–387
- Si W, Lei W, Zhang Y, Xia M, Wang F, Hao Q (2012) Electrodeposition of graphene oxide doped poly(3, 4-ethylenedioxythiophene) film and its electrochemical sensing of catechol and hydroquinone. *Electrochim Acta* 85:295–301
- Shaikh A, Saha S, Bakshi P, Hussain A, Ahammad AS (2013) Poly(brilliant cresyl blue)-modified electrode for highly sensitive and simultaneous determination of hydroquinone and catechol. *J Electrochem Soc* 160(4):B37–B42
- Huang X, Li Y, Chen Y, Wang L (2008) Electrochemical determination of nitrite and iodate by use of gold nanoparticles/poly(3-methylthiophene) composites coated glassy carbon electrode. *Sens Actuators B* 134(2):780–786
- Ba X, Luo L, Ding Y, Liu X (2013) Determination of tryptophan in the presence of ascorbic acid and dopamine using poly(sulfosalicylic acid) modified glassy carbon electrode. *Sens Actuators B* 187:27–32
- Zhang X, Gu S et al (2014) Simultaneous detection of roxithromycin and dopamine using a sensor platform based on poly(sulfosalicylic acid) and its application in human serum studies. *Anal Methods* 6(10):3316–3321
- Feng LJ, Zhang XH et al (2011) An electrochemical sensor based on single-stranded DNA–poly(sulfosalicylic acid) composite film for simultaneous determination of adenine, guanine, and thymine. *Anal Biochem* 419(2):71–75
- Li J, Chen J et al (2011) Determination of dopamine with improved sensitivity by exploiting an accumulation effect at a nano-gold electrode modified with poly(sulfosalicylic acid). *Microchim Acta* 174(3–4):345–352
- Li J, Kuang D, Feng Y, Zhang F, Xu Z, Liu M, Wang D (2012) Green synthesis of silver nanoparticles–graphene oxide nanocomposite and its application in electrochemical sensing of tryptophan. *Biosens Bioelectron* 42:198–206
- Liu S, Ou J, Wang J, Liu X, Yang S (2011) A simple two-step electrochemical synthesis of graphene sheets film on the ITO electrode as supercapacitors. *J Appl Electrochem* 41(7):881–884
- Kim YR, Bong S, Kang YJ, Yang Y, Mahajan RK, Kim JS, Kim H (2010) Electrochemical detection of dopamine in the presence of ascorbic acid using graphene modified electrodes. *Biosens Bioelectron* 25(10):2366–2369
- Li F, Li J, Feng Y, Yang L, Du Z (2011) Electrochemical behavior of graphene doped carbon paste electrode and its application for sensitive determination of ascorbic acid. *Sens Actuators B* 157(1):110–114
- Fang Y, Guo S, Zhu C, Zhai Y, Wang E (2010) Self-assembly of cationic polyelectrolyte-functionalized graphene nanosheets and gold nanoparticles: a two-dimensional heterostructure for hydrogen peroxide sensing. *Langmuir* 26(13):11277–11282
- Kim SK, Kim D, Jeon S (2012) Electrochemical determination of serotonin on glassy carbon electrode modified with various graphene nanomaterials. *Sens Actuators B* 174:285–291
- Ge S, Yan M, Lu J, Zhang M, Yu F, Yu J, Song X, Yu S (2012) Electrochemical biosensor based on graphene oxide–Au nanoclusters composites for L-cysteine analysis. *Biosens Bioelectron* 31(1):49–54
- Cui F, Zhang X (2012) Electrochemical sensor for epinephrine based on a glassy carbon electrode modified with graphene/gold nanocomposites. *J Electroanal Chem* 669:35–41
- Xu M, Zhu J, Su H, Dong J, Ai S, Li R (2012) Electrochemical determination of methyl parathion using poly(malachite green)/

- graphene nanosheets–nafion composite film-modified glassy carbon electrode. *J Appl Electrochem* 42(7):509–51627
31. Radoi A, Obreja AC, Eremia SA, Bragaru A, Dinescu A, Radu GL (2013) L-Lactic acid biosensor based on multi-layered graphene. *J Appl Electrochem* 43(10):985–994
 32. Wang Q, Kaminska I, Niedziolka Jonsson J, Opallo M, Li M, Boukherroub R, Szunerits S (2013) Sensitive sugar detection using 4-aminophenylboronic acid modified graphene. *Biosens Bioelectron* 50(0956–5663):331–337
 33. Xu Y, Bai H, Lu G, Li C, Shi G (2008) Flexible graphene films via the filtration of water-soluble noncovalent functionalized graphene sheets. *J Am Chem Soc* 130(18):5856–5857
 34. Yu Y, Chen Z, Zhang B, Li X, Pan J (2013) Selective and sensitive determination of uric acid in the presence of ascorbic acid and dopamine by PDDA functionalized graphene/graphite composite electrode. *Talanta* 112:31–36
 35. Fang Y, Guo S, Zhu C, Zhai Y, Wang E (2010) Self-assembly of cationic polyelectrolyte-functionalized graphene nanosheets and gold nanoparticles: a two-dimensional heterostructure for hydrogen peroxide sensing. *Langmuir* 26(13):11277–11282
 36. Huang X, Li Z, Zhang X, He X, Lin S (2013) Preparation of Pt/{PDDA-GN/PSS-GN}_n multilayer films and their electrocatalytic activity regarding methanol oxidation. *J Colloid Interface Sci* 393:300–305
 37. Zhao H, Zhang Y, Yuan Z (2001) Study on the electrochemical behavior of dopamine with poly(sulfosalicylic acid) modified glassy carbon electrode. *Anal Chim Acta* 441(1):117–122
 38. Hummers WS Jr, Offeman RE (1958) Preparation of graphitic oxide. *J Am Chem Soc* 80(6):1339
 39. Tuinstra F, Koenig JL (1970) Raman spectrum of graphite. *J Chem Phys* 53:1126
 40. Zhao DM, Zhang XH, Feng LJ, Jia L, Wang SF (2009) Simultaneous determination of hydroquinone and catechol at PASA/MWNTs composite film modified glassy carbon electrode. *Colloids Surf B* 74(1):317–321
 41. Kalimuthu P, John SA (2009) Nanostructured electropolymerized film of 5-amino-2-mercapto-1, 3, 4-thiadiazole on glassy carbon electrode for the selective determination of L-cysteine. *Electrochem Commun* 11(2):367–370
 42. Tehrani R, Ghadimi H, Ghani SA (2012) Electrochemical studies of two diphenols isomers at graphene nanosheet–poly(4-vinyl pyridine) composite modified electrode. *Sens Actuators B* 177:612–619
 43. Gan T, Sun J, Huang K, Song L, Li Y (2012) A graphene oxide–mesoporous MnO₂ nanocomposite modified glassy carbon electrode as a novel and efficient voltammetric sensor for simultaneous determination of hydroquinone and catechol. *Sens Actuators B* 177:412–418
 44. Liu W, Li C, Tang L, Tong A, Gu Y, Cai R, Zhang L, Zhang Z (2013) Nanopore array derived from L-cysteine oxide/gold hybrids: enhanced sensing platform for hydroquinone and catechol determination. *Electrochim Acta* 88:15–23